THE ASTROPHYSICAL JOURNAL, 328:600–609, 1988 May 15

RADIO EMISSION FROM CONICAL JETS ASSOCIATED WITH X-RAY BINARIES

R. M. HJELLMING
National Radio Astronomy Observatory[1]

AND

K. J. JOHNSTON
E. O. Hulburt Center for Space Research, Naval Research Laboratory
Received 1987 August 10; accepted 1987 November 5

ABSTRACT

Kinematic and physical models for the evolution of synchrotron radio emission in conical twin jets are derived and are shown to have most of the characteristics needed to explain the wide variety of radio properties in X-ray binaries: the spatial distribution of SS 433's radio jets; periodic emission from LSI +61°303 and quiescent Cyg X-3; and the stable quiescent emission from Cyg X-1, Cyg X-2, and Sco X-1. These models assume adiabatic expansion and are distinguished from other jet models by the dominance of lateral motions due to free or slowed expansion of a collimated flow of a hot, X-ray emitting gas. A laterally expanding environment, behaving like a supernova remnant expanding in a cylindrical geometry, is the location of steady production of relativistic plasma, and, when the relativistic plasma pressure is dominant, this geometry can provide the spherically expanding plasmoids causing radio flares.

Subject headings: radiation mechanisms — stars: individual (SS 433) — stars: radio radiation — X-rays: binaries

I. INTRODUCTION

The jets in SS 433 are understood better than those in any other radio-emitting X-ray binary because of their reliable behavior as twin corkscrews at radio (Hjellming and Johnston 1981*a*, 1981*b*, 1982, 1986; Schilizzi *et al.* 1982, 1984), optical (Margon 1984), and X-ray (Watson *et al.* 1983; Stewart and Watson 1986) wavelengths. The omnipresence of optically thin synchrotron emission, with spectral indices between −0.6 and −0.8 even during brief flaring episodes, led Hjellming and Johnston (1986) to suggest that the radio emission might originate in a "cylindrical" sheath around a gaseous jet that expands laterally into the surrounding medium with a Mach number of the order of 40.

The purpose of this paper is to examine the radio emission characteristics of conical jets with large Mach numbers, to solve the radiative transfer equations for adiabatically expanding sheaths of relativistic plasma, and to consider the effects of additional spherical bubbles of radio-emitting plasma produced when the relativistic plasma pressure becomes dominant. This combination of jet kinematics and evolution of the radio-emitting regions provides a basic model for explaining not only the SS 433 jets, but also the quiescent and sometimes periodic emission from other X-ray binaries. We conclude that while production of relativistic plasma is still the most fundamental and least understood part of the problem, geometry is important and that some of the characteristics of radio-emitting X-ray binaries can be understood by a mixture of the kinematic and physical behavior of radio emission produced in conical jet environments.

II. TWIN-JET KINEMATICS AND RADIATIVE TRANSFER

Let us consider twin jets with velocity vectors directed oppositely along an axis that can be described in terms of rotation about a direction fixed in space. Although we will utilize the geometric definitions used for the "precessing" jets of SS 433, the kinematic equations describe the general case of revolution about any axis fixed in space, so the models will describe jets with directions that change because of either precession or orbital motion, but not both. The combination of both is much more complicated and introduces too many geometrical parameters for the simple models discussed in this paper.

The conical jet geometry is shown in Figure 1*a*. The z-axis is shown as the direction of ejection of the twin jets, and each jet is assumed to have lateral expansion in the perpendicular direction with coordinates described by r. We will assume that the radio-emitting plasma is located between an inner radius r_1 and an outer radius r_2. Since we will consider only the simplified problem where the relativistic plasma has already been produced in conically expanding sheaths near the origin of the twin jets, we will impose boundary conditions on the radio-emitting plasma and magnetic field at a location z_0 from the origin, where the radius of the jet is r_0 at a time t_0. In Figure 1*b* we show a cross section perpendicular to the z-axis for each jet, indicating the inner and outer radii of the radio-emitting material and the geometry of the two interesting line-of-sight paths for directions perpendicular to the jets; a is the distance of the line of sight from the center of the jet and s is a segment of line-of-sight path length, so that the path length through the emitting regions is $L = 2(r_2^2 - a^2)^{1/2}$ for $a \geq r_1$ and $L = 2[r_2^2 - a^2)^{1/2} - (r_1^2 - a^2)^{1/2}]$ for $a < r_1$.

We will assume that the emission and absorption coefficients are appropriate to that of synchrotron emission from relativistic particles moving in what is, on average, random directions in what are, on average, randomly directed magnetic fields of average strength H. By also assuming a power-law energy spectrum of the form $N(E) = KE^{-\gamma}$, where γ is a constant, we can write the

[1] The National Radio Astronomy Observatory is operated by Associated Universities, Inc., under contract with the National Science Foundation.

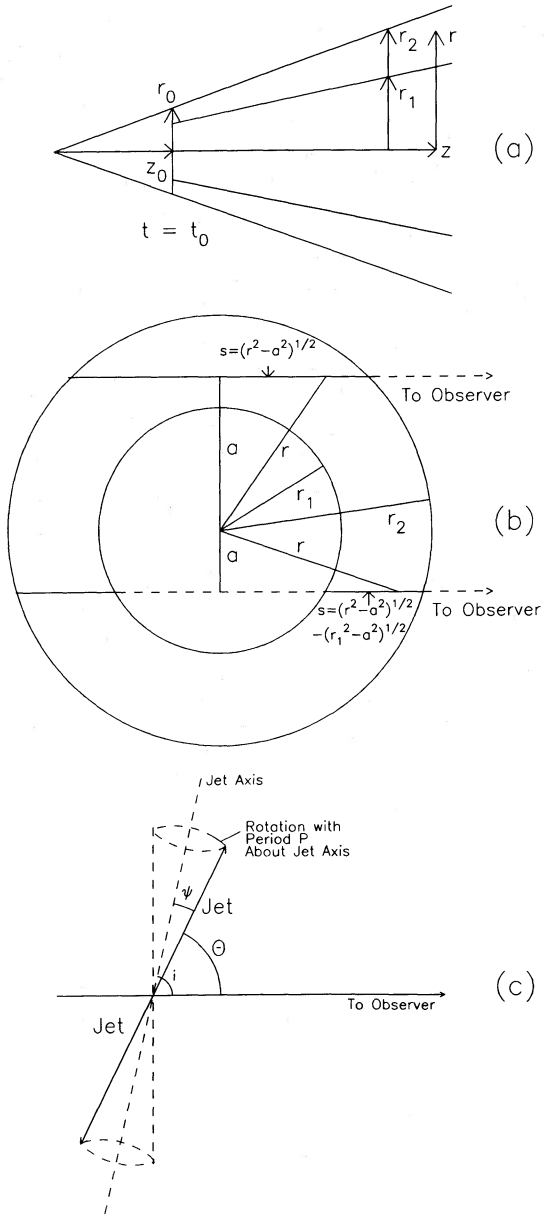

FIG. 1.—Three views of the geometry of adiabatically expanding twin conical jets: (*a*) a cross section of the lateral expansion in r and z in which boundary conditions are specified at $t = t_0$ when the ejected material is at a distance z_0 from the center and has a radius r_0, with inner radius r_1, and outer radius r_2 for the radio emitting region; (*b*) the cross section of the jet model seen perpendicular to the jet axis, indicating the line-of-sight path length as a function of distance from the center of the jet; and (*c*) the twin jet cones are shown in another perspective in which the jet z-axis is rotating about another axis with an angle Θ with respect to an observer.

emission and absorption coefficients as (Ginzburg and Syrovatskii 1965)

$$j_\nu \rho = j_0 \rho_0 (K/K_0)(H/H_0)^{(\gamma+1)/2}(\nu/\nu_0)^{-(\gamma-1)/2} , \tag{1}$$

and

$$\kappa_\nu \rho = \kappa_0 \rho_0 (K/K_0)(H/H_0)^{(\gamma+2)/2}(\nu/\nu_0)^{-(\gamma+4)/2} . \tag{2}$$

This leads to a simple expression for the radiative transfer source function,

$$j_\nu/\kappa_\nu = (2kT_0/\lambda_0^2)(H/H_0)^{-1/2}(\nu/\nu_0)^{5/2} , \tag{3}$$

if we define a brightness temperature T_0 for a reference wavelength λ_0 (and frequency ν_0) in terms of the conditions at t_0 where we specify a magnetic field H_0 and a density coefficient K_0 for relativistic plasma. Defining the optical depth for a line of sight of length $L = L(a)$ perpendicular to the z-axis to be $\tau_\nu(a) = \kappa_\nu \rho L$ and assuming that at any z the values K, H, etc., are uniform across the

conical jet, the specific intensity is

$$I_\nu(a, z) = (2kT_0/\lambda_0^2)(H/H_0)^{-1/2}(\nu/\nu_0)^{5/2}[1 - \exp(-\kappa_\nu \rho L/\sin\Theta)] \quad (4)$$

for an observer for whom the jet is seen with an angle Θ with respect to the their line of sight. If we define an optical depth scaling parameter, $\tau_0 = 2\kappa_0 \rho_0 r_0$, then

$$\tau_\nu(a) = \tau_0(K/K_0)(H/H_0)^{(\gamma+2)/2}(\nu/\nu_0)^{-(\gamma+4)/2}[L/(2r_0 \sin\Theta)] , \quad (5)$$

and the contribution to the flux density of a cross section of the jet of radius r_2 and length dz is then

$$dS_\nu(z)/dz = \sin\Theta \int I_\nu(a, z)da = (S_0/r_0)(\nu/\nu_0)^{5/2} \sin\Theta \int_0^{r_2} (H/H_0)^{-1/2}\{1 - \exp[-\tau_\nu(a)]\}d(a/r_0) , \quad (6)$$

where we have defined $S_0 = (2kT_0/\lambda_0^2)\pi(r_0/d)^2$, with d being the distance to the object. Examining equations (5) and (6), we see that if we can specify the variation of H/H_0 and K/K_0 with z, the radio-emitting characteristics of the conical jet are determined by the boundary-condition parameters, S_0 and τ_0, and the angle Θ with respect to the observer's line of sight.

The variation of Θ as a function of time t can be described (Hjellming and Johnston 1981*a*) by

$$\cos\Theta = \cos i \cos\psi \cos[2\pi(t - t_{\rm ref})/P] + \sin i \sin\psi , \quad (7)$$

where ψ is the angle the jets maintain with respect to the axis about which they rotate with a period P, i is the angle between the rotation axis and the observer's line of sight, and $t_{\rm ref}$ is a reference time for the jet kinematics. The geometry defining the variation of Θ is shown schematically in Figure 1*c*. For SS 433, $i = 80°$, $\psi = 20°$, and $P = 162.5$ days.

Equations (5) and (6) describe the emission profile as a function of z in each of the twin jets. It is obviously dependent upon $\sin\Theta$, except in the portions of the jet that are optically thin. We can make this profile strictly a function of z by specifying the variation of H/H_0 and K/K_0 with z. If we assume that the ejection of jet material is continuous and unimpeded in the z-direction so that dz/dt is constant everywhere in the jet, that is, there are no velocity gradients along the z-axis, then the jet can only expand perpendicular to the jet axis. Under these circumstances the conservation of magnetic flux requires that $H = H_0(r_2/r_0)^{-1}$. Further, if we assume that the expansion with r_2 is adiabatic, then conservation of both the total energy and the number of relativistic particles requires that $E = E_0(r_2/r_0)^{-2/3}$ and $K = K_0(r_2/r_0)^{-2(\gamma+2)/3}$. When adiabatic expansion is constrained to two dimensions, one has a more gradual decline of emission from the relativistic plasma than found with three-dimensional adiabatic expansion. Using these dependencies upon the expansion parameter r_2/r_0, equation (5) becomes

$$\tau_\nu = \tau_0(r_2/r_0)^{-(7\gamma+8)/6}(\nu/\nu_0)^{-(\gamma+4)/2}[L/(2r_2 \sin\Theta)] = \tau'_\nu[L/(2r_2)] , \quad (8)$$

where

$$\tau'_\nu = \tau_{\nu 0}(r_2/r_0)^{-(7\gamma+8)/6}/\sin\Theta , \qquad \tau_{\nu 0} = \tau_0(\nu/\nu_0)^{-(\gamma+4)/2} .$$

Then

$$dS_\nu(z)/dz = (S_0/r_0)(\nu/\nu_0)^{5/2} \sin\Theta(r_2/r_0)^{3/2} \int_0^1 [1 - \exp(-\tau_\nu)d(a/r_2) , \quad (9)$$

(cf. eq. [6]), which can be integrated to obtain

$$dS_\nu(z)/dz = (S_0/r_0)(\nu/\nu_0)^{5/2} \sin\Theta(r_2/r_0)^{3/2}[1 - \exp(-\tau'_\nu)]\xi_2(\tau'_\nu, r_1/r_2) , \quad (10)$$

where we have defined and the geometrical correction function

$$\xi_2(\tau'_\nu, u_1) = \frac{\int_0^{u_1} [[1 - \exp - \tau'_\nu[(1 - u^2)^{1/2} - (u_1^2 - u^2)^{1/2}]]du + \int_{u_1}^1 \{1 - \exp[-\tau'_\nu(1 - u^2)^{1/2}]\}du}{1 - \exp(-\tau'_\nu)} , \quad (11)$$

in which $u = a/r_2$ and $u_1 = r_1/r_2$. The function ξ_2 varies between unity in the optically thick limit and $(\pi/4)[1 - (r_1/r_2)^2]$ in the optically thin limit. Plots of ξ_2 as a function of τ'_ν for a range of values of u_1 are shown in Figure 2*a*.

Equation (10) can be integrated over z from z_0 to ∞ to obtain the flux density contributed by the jet. For the case of "free expansion" we have both dz/dt and dr_2/dt constant, so $z = z_0(t/t_0) = z_0\zeta$ and $r_2 = r_0(z/z_0) = r_0\zeta$ if we define $\zeta = z/z_0 = t/t_0$. If lateral expansion is slowed by expansion into a medium of constant density, then $r_2 = r_0(z/z_0)^p = r_0\zeta^p$, where $p = \frac{1}{2}$ for adiabatic (energy conserving) expansion and $p = \frac{1}{3}$ for expansion with conservation of momentum. These types of slowed expansion are analogous to the $t^{2/5}$ and $t^{1/4}$ phases of expansion of explosions (like supernova ejecta) into a constant density medium. In order to simplify the present discussion we will use $p = \frac{1}{2}$ as representative of slowed expansion, so that $p = 1$ and $\frac{1}{2}$ lead to the different solutions for the properties of the jets which we will call the free- and slowed-expansion cases, respectively.

If we define an initial Mach number for the jets, $M_0 = z_0/r_0$, and take the constant δ to be 0 for the free-expansion case and 1 for the slowed-expansion case, then we can write the solution for the flux density from z_0 to z for both jets as

$$S_\nu(<z) = 2M_0 S_0(\nu/\nu_0)^{5/2} \sin\Theta \int_1^{z/z_0} \zeta^{3/(2+2\delta)}[1 - \exp(-\tau'_\nu)]\xi_2(\tau'_\nu, r_1/r_2)d\zeta , \quad (12)$$

where

$$\tau'_\nu = \tau_{\nu 0}\zeta^{-(7\gamma+8)/(6+6\delta)} , \quad (13)$$

with $\tau_{\nu 0} = \tau_0(\nu/\nu_0)^{-(\gamma+4)/2}/\sin\Theta$.

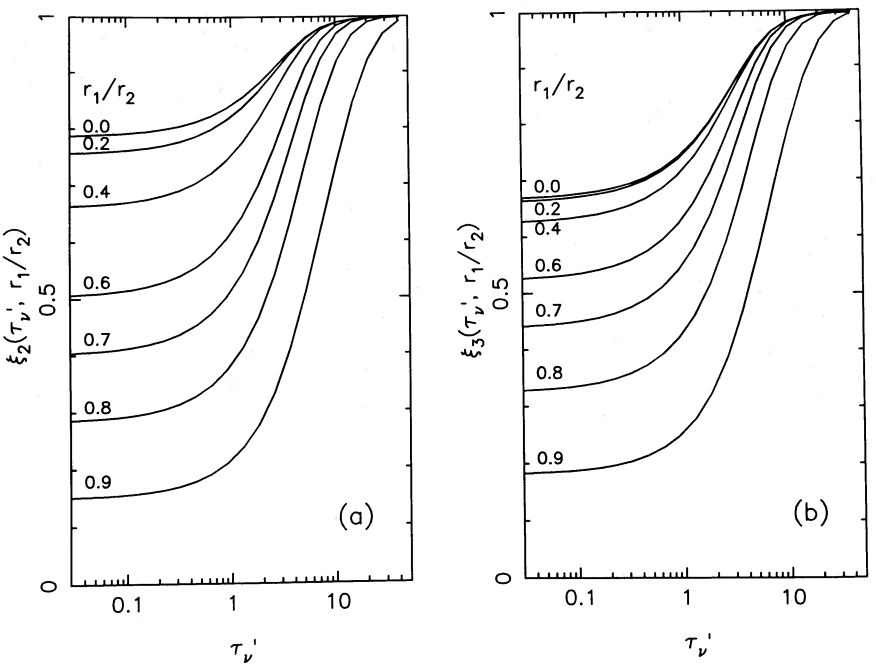

FIG. 2.—Geometrical correction functions (*a*) $\xi_2(\tau_\nu', r_1/r_2)$ and (*b*) $\xi_3(\tau_\nu', r_1/r_2)$ for conical (or cylindrical) and spherical geometries are plotted as functions of the optical depth variable τ_ν' for several values of r_1/r_2.

Examination of equation (12) reveals that $dS_\nu/d\zeta$, which we will call the jet-profile function, has optically thick and thin segments given by

$$(dS_\nu/d\zeta)_{\rm thick} = 2M_0 S_0 (\nu/\nu_0)^{5/2} \sin\Theta \zeta^{3/(2+2\delta)} , \tag{14}$$

and

$$(dS_\nu/d\zeta)_{\rm thin} = 2M_0 S_0 \tau_0 (\nu/\nu_0)^{-(\gamma-1)/2} (\pi/4)[1-(r_1/r_2)^2]\zeta^{-(7\gamma-1)/(6+6\delta)}$$

that have intersection points that define $\zeta_m = z_m/z_0 = t_m/t_0$. The flux density profile reaches a maximum at

$$z_m/z_0 = \{(\pi/4)[1-(r_1/r_2)^2]\tau_0/\sin\Theta\}^{(6+6\delta)/(7\gamma+8)} (\nu/\nu_0)^{-(\gamma+4)(3+3\delta)/(7\gamma+8)} , \tag{15}$$

which determines not only a size scale for the maximum contribution to the flux density of the jet, but also the observed size scale of the jets for a given dynamic range in a radio image. If $I_{\rm min}/I_{\rm max}$ specifies this dynamic range, then the observed angular size of the twin-jet system is

$$\Theta_{\rm jet} \approx 2(z_m/d) \sin\Theta (I_{\rm min}/I_{\rm max})^{-(6+6\delta)/(7\gamma-1)} \tag{16}$$

because $\Theta_m = (2z_m \sin\Theta)/d$ is the apparent angular separation between the twin-jet maximum intensities, and from equation (14),

$$I_{\rm min}/I_{\rm max} \approx (\Theta_{\rm jet}/\Theta_m)^{-(7\gamma-1)/(6+6\delta)} .$$

Integration of equation (12) from z_0 to ∞ gives an optically thin limit of

$$(S_\nu)_{\rm thin} = 2M_0 S_0 \tau_0 (\nu/\nu_0)^{-(\gamma-1)/2} (\pi/4)[1-(r_1/r_2)^2](6+6\delta)/[7(\gamma-1)] \tag{17}$$

whenever τ_0 is small enough so that the outer, optically thin, portions of the jets predominate. On the other extreme, integration of equation (12) gives an optically thick limit, if the optically thin portions of the jet provide a negligible portion of the flux, which is

$$(S_\nu)_{\rm thick} = 2M_0 S_0 (6+6\delta)/(15+6\delta)(\tau_0/\sin\Theta)^{(15+6\delta)/(7\gamma+8)} (\nu/\nu_0)^{[10(\gamma-1)-3(\gamma+4)\delta]/[7\gamma+8]} . \tag{18}$$

We see that in cases where the optically thick portions of the jets contribute significantly, there should be a modulation of that component of the radio emission whenever Θ changes as a function of time. If there is no variation of Θ with time, then this model produces jets with a stable level of radio emission.

In Figure 3 we plot examples of the flux density profile of conical jets as a function of $z/z_0 = t/t_0$ for $\nu = \nu_0$ (*dotted lines*), $\nu_0/2$, $\nu_0/4$, $\nu_0/8$, and $\nu_0/16$ (*solid lines*). Figures 3*a* and 3*b* show the cases of free ($\delta = 0$) and slowed ($\delta = 1$) expansion, respectively, for $\gamma = 3$, $\Theta = 90°$, and $\tau_0 = 10$ in the form of plots of $dS_\nu/d\zeta$ versus ζ. Figures 3*c* and 3*d* show plots of $S_\nu(<z)$ versus ζ that more clearly show the contributions to the radio emission structure of the jets and the much larger size scale for the "slowed" cases. Figures 3*a* and 3*b* can be viewed as showing the jet-profile function for smaller values of τ_0 since the curves are the same except for truncation at the left side that moves progressively to the right as τ_0 decreases.

Figures 4*a* and 4*b* show the radio spectra in the form of log S_ν versus ν plots for τ_0 ranging in factors of 10 from 10^3 down to 10^{-4}

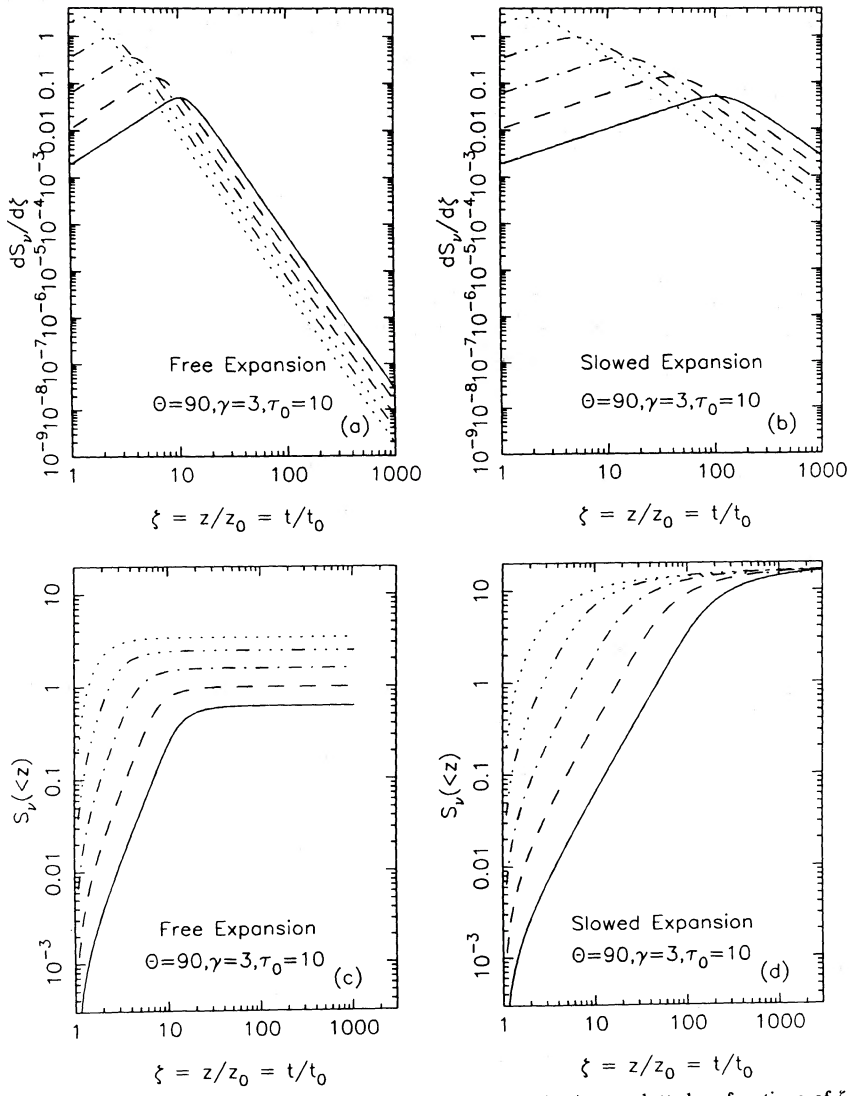

FIG. 3.—The jet-profile function $dS_\nu/d\zeta$ and the cumulative flux density from z_0 to z, $S_\nu(<z)$, are plotted as functions of $\zeta = z/z_0 = t/t_0$ for both free- and slowed-expansion conical-jet models with $\gamma = 3$, $\tau_0 = 10$, and a fixed $\Theta = 90°$. The curves are for frequencies differing by factors of 2 from $\nu = \nu_0$ (*dotted line*) to $\nu = \nu_0/16$ (*solid line*).

for the case of $\gamma = 3$ and the assumptions of free and slowed expansion, respectively. In the optically thin limit we have source spectra with $\alpha_{\rm thin} = -(\gamma - 1)/2$, the well-known result for synchrotron radiation sources. However, for large values of τ_0 the spectral index is $\alpha_{\rm thick} = [10(\gamma - 1) - 3(\gamma + 4)\delta]/(7\gamma + 8)$, and for the $\gamma = 3$ case this gives $\alpha_{\rm thick} = 0.69$ and -0.0345 for the free- and slowed-expansion cases, respectively. The flattening of the spectra that occurs for the cases of slowed expansion is of particular interest; one obtains $\alpha_{\rm thick} = 0$ for $\gamma = 3.14$.

It is implicit in the foregoing model that the contributions of optically thick sections of conical jets to observable radio emission will vary if Θ varies due to changes in the jet geometry. In Figure 5 we show three cases that may be of particular interest. In Figure 5*a* we show the variations in radio spectrum for a nearly optically thick jet with $\tau_0 = 1$, $\gamma = 3$, and slowed expansion. This is close to the modulation that might occur for an X-ray binary like Cyg X-1, which has a nearly flat spectrum most of the time. Figure 5*b* shows a marginally optically thick case with $\gamma = 3$, $\tau_0 = 0.01$, and free lateral expansion; it is of interest because it approximates some of the behavior of the quiescent Cyg X-3 (Hjellming 1976). Finally, Figure 5*c* shows a slightly more optically thin case of free expansion with $\tau_0 = 0.001$; this approximates some of the behavior of LSI $+61°303$, an X-ray binary which periodically varies between optically thin and optically thick states. In all three cases the similarity of behavior is suggestive, but a firm conclusion about whether these models are consistent with the behavior of these sources requires either much more detailed comparison with available data, or much more detailed data, than is appropriate for discussion in this paper.

The case of SS 433, which was the initial motivation for the conical jet model that we have discussed, is the only one where images of extended emission allow a comparison of observations with the extended structures predicted by the model. A model with $\tau_0 = 0.0001$ and $\gamma = 2.32$ easily matches the dominant spectral behavior of SS 433; however, it is the required assumptions concerning slowed or free lateral expansion that are most interesting. In Figure 6 we show three images corresponding to complete free expansion (Fig. 6*a*), slowed expansion out to $\zeta = 90$ with free expansion after that point (Fig. 6*b*), and slowed expansion

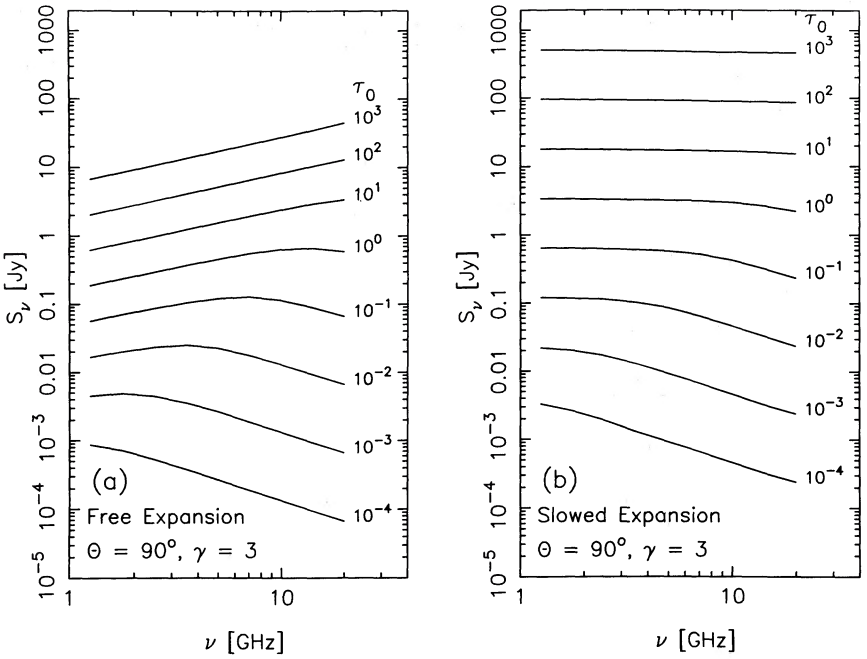

FIG. 4.—The radio spectra, in the form of plots of S_ν vs. ν, are presented for $\tau_0 = 10^3$, 10^2, 10^1, 10^0, 10^{-1}, 10^{-2}, 10^{-3}, and 10^{-4} for both (*a*) free and (*b*) slowed expansion. All models have $\gamma = 3$, $\Theta = 90°$, and $\nu_0 = 20$ GHz.

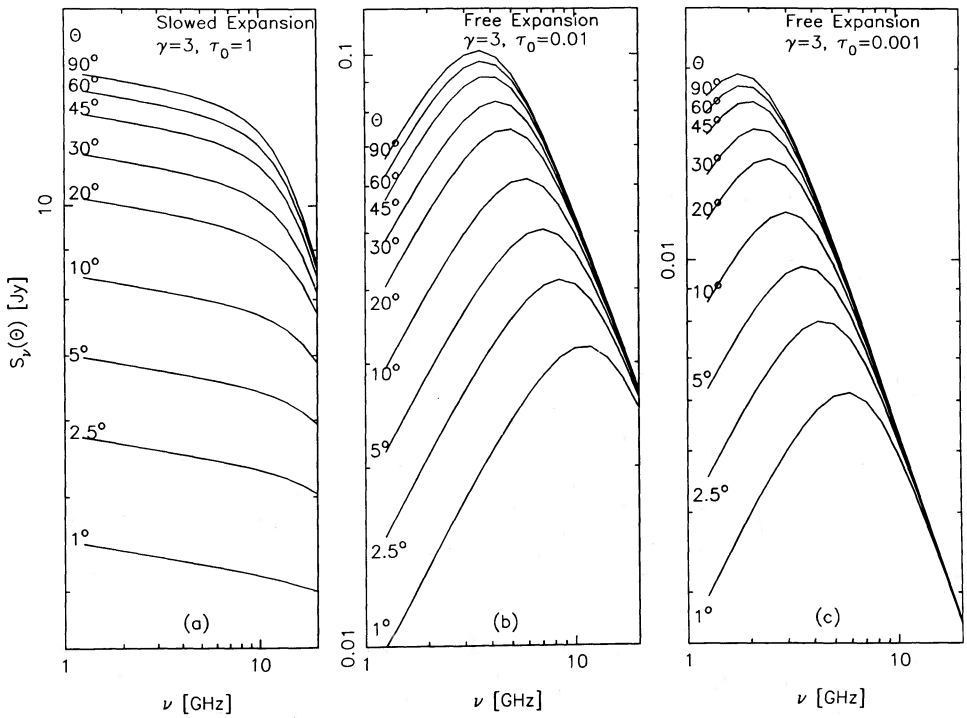

FIG. 5.—Radio spectra for $\Theta = 1$, 2.5, 5, 10, 20, 30, 45, 60, and 90° are given for $\gamma = 3$. The three cases show some of the behavior of Cyg X-1, quiescent Cyg X-3, and LSI +61°303, respectively: (*a*) $\tau_0 = 1$ with slowed expansion; (*b*) $\tau_0 = 0.01$ with free expansion; and (*c*) $\tau_0 = 0.001$ with free expansion.

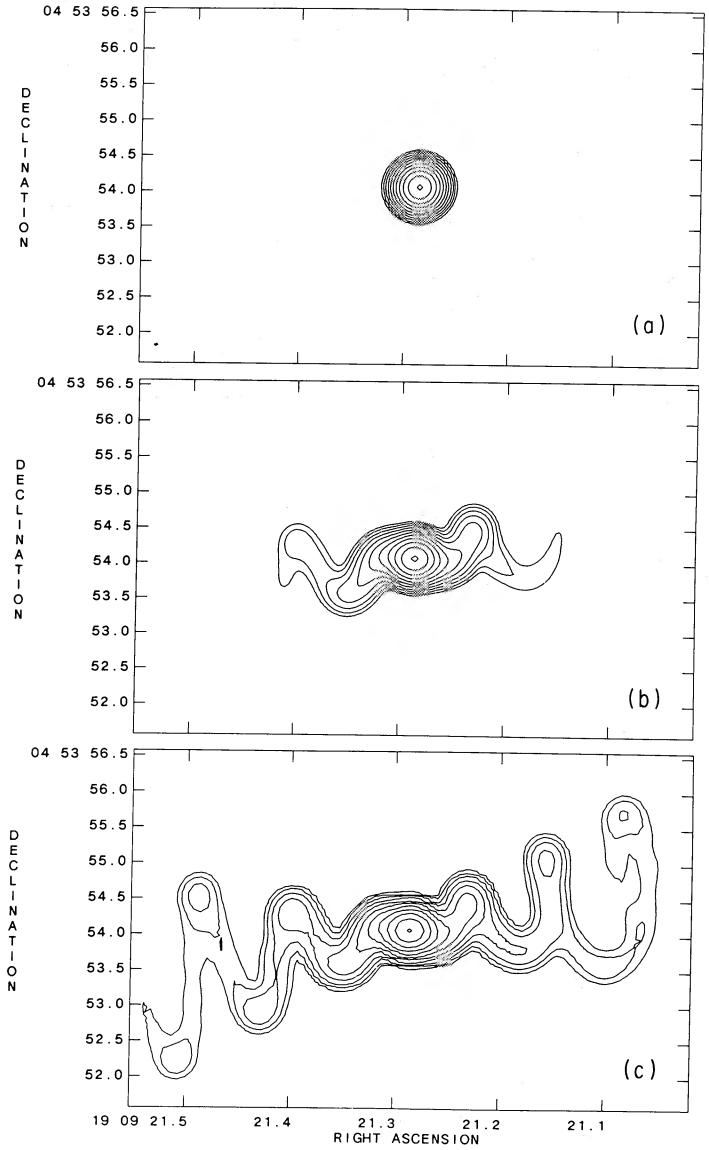

FIG. 6.—Three images correspond to the parameters that are typical of the extended ratio jets of SS 433: (*a*) the case assuming free expansion, (*b*) the case where slowed expansion occurs out to $\zeta = z/z_0 = t/t_0 = 90$ and then becomes free expansion, and (*c*) the case of slowed expansion. Contours range in factors of 2 from 10^{-3} of the peak on up, and the models have been convolved with the 0".33 beam of the 35 km VLA at 5 GHz. The middle (*b*) image is similar to all of the 5 GHz images of SS 433 (Hjellming and Johnston 1981*a*, 1981*b*, 1983, 1986).

throughout the jet (Fig. 6*c*). All images have been convolved with a point spread function corresponding to the 5 GHz resolution of the 35 km VLA. Although we will defer to another paper the detailed comparisons of some 30 epochs of VLA images of SS 433 with conical jet models, some simple conclusions can be drawn from Figure 6. Jets with free lateral expansion throughout do not exhibit the greater than 0".1 extended structure seen in SS 433—such jets can be seen only with VLBI resolution. Similarly there has been no case in the SS 433 images from 1979 through 1986 in which one sees the slow decays that would give as many observable "loops of the corkscrew"—as shown in the slowed lateral—expansion model in Figure 6*c*. Only the central image in Figure 6*b*, a transition from slowed expansion to free expansion at $\zeta = 90$ matches the general appearance of the SS 433 images. In Figure 7 we show one case of a detailed comparison of the jet-profile function with a "break" at $\zeta = 90$ with the observed jet-profile intensity for an image at JD 2,444,589 (Hjellming and Johnston 1986). In addition to the need of an effect like the "break" to make the images "SS 433–like", the example in Figure 7 requires a very specific location for the break of transition from slowed expansion to free expansion.

III. EVOLUTION OF TWIN BUBBLES OF RADIO EMISSION

From the previous discussion it is obvious that any changes in K_0 and/or H_0 as functions of time will also produce time-dependent effects in the total radio emission from the jet. One obvious extreme will occur when the values of these parameters lead to dominance of the pressure of relativistic electrons. Under those circumstances twin spherical bubbles of relativistic electrons and magnetic fields will evolve as independent plasmoids with initial translational velocities in the z-direction; in this extreme such

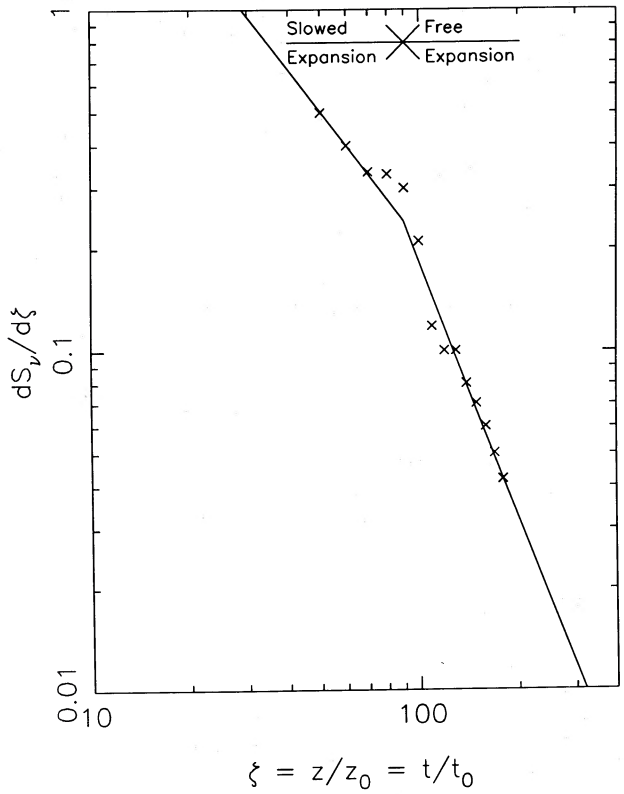

FIG. 7.—SS 433 theoretical jet-profile function, $dS_\nu/d\zeta$, with a transition from slowed to free expansion at $\zeta = z/z_0 = t/t_0 = 90$ is compared with the observed 5 GHz jet profile obtained with a VLA image obtained on JD 2,444,589.

plasmoids can expand with the sound speed of the relativistic electrons, $c/3^{1/2}$, and then the twin bubbles may merge quickly into a single expanding sphere of radio-emitting plasma. Thus it is clearly possible that spherically expanding "events" can be "added" to the above model to explain the flaring events in X-ray binaries. Our working hypothesis is that the conical jet model is appropriate to relatively quiescent jets while additional spherically expanding bubbles correspond to flaring events.

Flaring on short time scales is one of the best known characteristics of radio-emitting X-ray binaries. It is therefore necessary to produce steady or periodic emission, the problem addressed in the previous section, and to produce a mechanism for transient flares. In this section we explore the working hypothesis that flaring events are a consequence of brief episodes of extremely efficient production of relativistic plasma at the base of conical jets resulting in rapid expansion of relativistic plasmoids with basically three-dimensional behavior. Relativistic plasmoids produced in this environment will expand with velocities between a lower limit set by the sound speed in the gas of the jets and an upper limit of $c/3^{1/2}$ corresponding to a purely relativistic gas with unimpeded expansion. For cases near the lower limit the relativistic plasma is closely tied to the gas jet as was assumed in the conical jet models in the previous section. For cases near the upper limit the plasmoids produced by the twin jets may merge quickly into a single relativistic plasmoid. For the intermediate cases one can have twin "bubbles" of relativistic plasma that move outward with the velocity of the jets but expand individually in three dimensions with no significant "jet" effect except their bulk motion along the z-axis. Let us proceed with the working hypothesis that we can model the spherical expansion of such plasmoids to add flaring behavior in the context of a conical twin-jet model.

All of the discussion in the previous section through equation (6) is valid for spherically expanding subcomponents. The geometry for each plasmoid will be spherical with radii and line-of-sight characteristics defined in Figure 1*b*. With expansion in three dimensions the conservation of magnetic flux requires that $H = H_0(r_2/r_0)^{-2}$. If the expansion is adiabatic, the conservation of both the total energy and the number of relativistic particles requires that particle energies vary as $E = E_0(r_2/r_0)^{-1}$, and the density coefficient for relativistic electrons varies as $K = K_0(r_2/r_0)^{-(\gamma+2)}$. In the spherically symmetric context each radio-emitting plasmoid will have a flux density given by $S_\nu = 2\pi(r_2/d)^2 \int_0^1 uI_\nu(u)du$ where $u = a/r_2$. In a manner analogous to that used in the previous section, we assume that the emitting region is located between radii r_1 and r_2. The optical depth for the spherical case is then

$$\tau_\nu = \tau_0(r_2/r_0)^{-(2\gamma+3)}(\nu/\nu_0)^{-(\gamma+4)/2}[L/(2r_2)] = \tau'_\nu[L/(2r_2)] , \tag{19}$$

and the flux density is given by

$$S_\nu(r_2) = 2\pi S_0(\nu/\nu_0)^{5/2}(r_2/r_0)^3[1 - \exp(-\tau'_\nu)]\xi_3(\tau'_\nu, r_1/r_2) , \tag{20}$$

where we now have a different (three-dimensional) geometrical correction function

$$\xi_3(\tau'_\nu, u_1) = \frac{\int_0^{u_1} [\![1 - \exp -\tau'_\nu[(1-u^2)^{1/2} - (u_1^2 - u^2)^{1/2}]]\!] u\,du + \int_{u_1}^1 \{1 - \exp[-\tau'_\nu(1-u^2)^{1/2}]\}u\,du}{\{0.5[1 - \exp(-\tau'_\nu)]\}} . \tag{21}$$

Figure 2*b* shows plots of ξ_3 as a function of τ'_ν for various values of $u_1 = r_1/r_2$. In the optically thick limit ξ_3 is unity, while in the optically thin limit it is equal to $(2/3)(1 - u_1^3)^{1/2}$.

With the exception of the geometrical correction function ξ_3, equations (20) and (21) correspond to the well-known solutions for the evolution of adiabatically expanding spheres (van der Laan 1966; Kellerman 1966), except we have not made the usual simplifying assumption whereby all lines of sight through the source have the same length L, but instead have defined the correction function ξ_3 which can reduce fluxes in the optically thin regime by up to $1 - (2/3)(1 - u_1^3)^{1/2}$. This correction function has the most effect when comparing fluxes for sources that are in the transition phase from optically thick to optically thin. In defining ξ_3, we have allowed for the possibility that the radio emission occurs only in a spherically symmetric shell. Figure 8 shows plots of flux densities as a function of r_2/r_0 for ν_0, $\nu_0/2$, and $\nu_0/4$ for three cases: the solid lines correspond to $r_1/r_2 = 0$; the dotted lines correspond to the standard model where the line of sight path through the source is taken to be equal to the diameter of the spherically expanding bubble, that is $\xi_3 = 1$; and the dashed lines correspond to the case where $r_1/r_2 = 0.8$. One can see that the primary practical effect of the geometry correction function occurs in determining spectral indices during the transition phases from optically thick to optically thin.

The observational signatures of twin expanding bubbles are identical to those of the standard models (van der Laan 1966; Kellerman 1966) except for the altered ratios between the optically thick and both the maxima and optically thin parts of the light curves. Thus the well-established matching of such models and the large flares of Cyg X-3 is preserved. The other point that we wish to argue is that the conical jet geometry may play a major role in not only quiescent/periodic emission, but also provides another geometry for the generation of relativistic particle plasmoids that is an alternative to requiring the frequent production of shock acceleration regions in spherically symmetric geometries. Both possibilities should be considered in future interpretation of radio flares in Cyg X-3 and other flaring X-ray binaries.

The evolution of conical jets can be affected by the presence of thermal plasma that contributes significantly to the radiative transfer. It is well known (Seaquist *et al.* 1974; Marscher and Brown 1975) that some Cyg X-3 flaring events have significant and evolving depolarization by coexisting thermal plasma. It is straightforward to include these effects, as shown by Marscher and Brown (1975). If the temperature of the coexisting thermal plasma can be assumed to be constant, then the equations for the mass absorption and emission coefficients have the additional terms $(\kappa_0 \rho_0)_{ff}(r_2/r_0)^{-2}(\nu/\nu_0)^{-2.11}$ and $(j_0 \rho_0)_{ff}(r_2/r_0)^{-2}(\nu/\nu_0)^{-0.11}$, respectively, for the cylindrical geometry assumed in § II; for the spherical geometry discussed in § III these coefficients are proportional to $(r_2/r_0)^{-3}$. Two more parameters are therefore introduced into the problem. Because of the different dependence upon r_2 of the free-free and synchrotron coefficients the relative dominance of two types of absorption can change in the jets. However, rather than expand the parameter space explored in this paper, we will defer the discussion of thermal plasma contributions to papers interpreting the observations for specific objects.

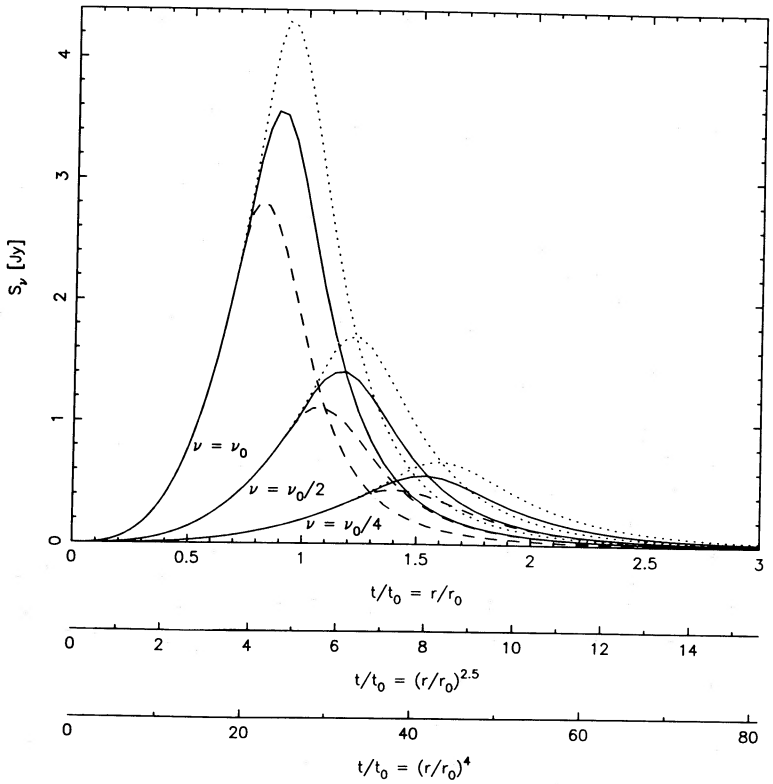

FIG. 8.—Models for the evolution of uniform, spherically symmetric synchrotron sources at frequencies of $\nu = \nu_0$, $\nu_0/2$, and $\nu_0/4$ are plotted for the following cases: (*solid lines*) the solutions derived from eq. (21) with $r_1/r_2 = 1$; (*dotted lines*) the corresponding (van der Laan 1966; Kellermann 1966) models with $\xi_3 = 1$; and (*dashed lines*) the solutions from eq. (21) corresponding to $r_1/r_2 = 0.8$.

IV. CONCLUSIONS

Models of adiabatically expanding, synchrotron radiation-emitting conical jets may explain not only the SS 433 extended jets, but also some of the characteristics of radio emission from X-ray binaries. The models with optically thin parameters fit most of the behavior of SS 433. The transition from slowed to free lateral expansion indicates that the initial jets are slowed by a dense environment, but they "escape" from this environment ~ 100 days after ejection, that is at distances of ~ 25 light days. The model also indicates that the main feature that distinguishes SS 433 from the other radio-emitting X-ray binaries is the density and size of the large region of external gas that slows the lateral expansion of the jets. The models do not attempt to address the details of the acceleration regions, or the substructures seen at radio wavelengths with VLBI techniques. These models do account for both the spatial and temporal behavior of the SS 433 radio jets, and with smaller (or negligible) inner regions of "slowed" expansion may provide both an explanation for both stable (or periodic) radio emission and an alternate geometry for acceleration regions.

The physical conditions under which radio-emitting regions of relativistic plasma expand only laterally are tied clearly to cases where the basic jet phenomenon is a highly collimated, hot gas ejection along the axes of accretion disks. As long as the relativistic plasma is a "surface" phenomenon in the lateral expansion of the gaseous jets, it is logical for them to expand in only two dimensions. In this context the physics of the production of relativistic electrons is the two-dimensional equivalent of the well-known case of expansion of supernova remnants into the interstellar medium. In cases where the production of relativistic plasma is "more" efficient, at least locally, it is obvious that plasmoids dominated by relativistic particle pressure can occur, and that each of these plasmoids then may expand in three dimensions according to the classical models for such radio sources. Thus the model is a useful working hypothesis for explaining some quiescent radio phenomena in X-ray binaries, and also a geometry to be considered for the production of relativistic plasma for flaring events.

Obtaining stable synchrotron radiation-emitting sources with flat radio spectra, such as is well-known for Cyg X-1, has always been a problem for standard models. Thus it is fundamentally interesting that slowed, adiabatically expanding conical jets with $\gamma = 3.14$ are exactly flat-spectrum radio sources. It is also of interest that periodic modulation of optically thick portions of jets may play a role in cases where such variations occur. This does not exclude the possibility of periodic triggering of radio flares due to motion of the accretion disk into a denser environment. It does mean that one needs to make detailed observations to distinguish between the two models for periodic radio emission. Both geometric modulation of a steady conical-jet source and synchrotron flaring events triggered by special conditions at certain places in the binary orbit are possible, and both types of periodic modulation may occur.

In the last analysis the usefulness of this model, certainly in the case of the extended emission of SS 433, is that it provides a different, laterally expanding environment in which to obtain shocks or other phenomena that accelerate relativistic particles. In subsequent papers we will treat the gaseous jets and sheaths of relativistic plasma more realistically, with cooling and more correct gas dynamical treatment of shocks and interaction with the external medium that "slows" the expansion.

In the case of flat spectrum or periodic radio sources associated with X-ray binaries (Cyg X-1, quiescent Cyg X-3, LSI $+61°303$) these models for adiabatically expanding conical jets predict particular observational signatures in the radio spectra. If such signatures can be found, the observations will allow studies of the kinematics of new twin jets in a manner heretofore restricted to SS 433.

REFERENCES

Ginzburg, V. L., and Syrovatskii, S. I. 1965, *Ann. Rev. Astr. Ap.*, **3**, 297.
Hjellming R. M. 1976, NASA SP-389, p. 233.
Hjellming, R. M., and Johnston, K. J. 1981*a* *Nature*, **290**, 100.
———. 1981*b*, *Ap. J.* (*Letters*), **246**, L141.
———. 1982, in *Extragalactic Radio Sources* ed. D. S. Heeschen and C. M. Wade (Dordrecht: Reidel), p. 205.
———. 1986, in *Physics of Accretion onto Compact Objects*, ed. K. O. Mason, M. G. Watson, and N. E. White (Berlin: Springer), p. 287.
Kellermann, K. I. 1966, *Ap. J.*, **146**, 621.
Margon, B. 1984, *Ann. Rev. Astr. Ap.*, **22**, 507.
Marscher, A. P., and Brown, R. L. 1975, *Ap. J.*, **200**, 719.
Schilizzi, R. T., Fejes, I., Romney, J. D., Miley, G. K., Spencer. R. E., and Johnston, K. J. 1982, in *Extragalactic Radio Sources*, ed. D. S. Heeschen and C. M. Wade (Dordrecht: Reidel), p. 205.
Schilizzi, R. T., Romney, J. D., and Spencer, R. E. 1982, in *VLBI and Compact Radio Sources*, ed. R. Fanti, K. I. Kellerman, and G. Setti (Dordrecht: Reidel), p. 289.
Seaquist, E. R., Gregory, P. C., Perley, R. A., Becker, R. W., Carlson, J. B., Kundu, M. R., Bignell, R. C., and Dickel, J. R. 1974, *Nature*, **251**, 395.
Stewart, G. C., and Watson, M. G. 1986, in *Physics of Accretion onto Compact Objects*, ed. K. O. Mason, M. G. Watson, and N. E. White (Berlin: Springer), p. 303.
van der Laan, H. 1966, *Nature*, **211**, 1131.
Watson, M. G., Willingale, R., Grindlay, J. E., and Seward, F. D. 1983, *Ap. J.*, **273**, 688.

ROBERT M. HJELLMING: National Radio Astronomy Observatory, P.O. Box O, Socorro, NM 87801-0837

KENNETH J. JOHNSTON: Naval Research Laboratory, Code 4130, Washington, DC 20375